

Mechanistic Insights into the Brust–Schiffrin Two-Phase Synthesis of Organo-chalcogenate-Protected Metal Nanoparticles

Ying Li, Oksana Zaluzhna, Bolian Xu, Yuan Gao, Jacob M. Modest, and YuYe J. Tong*

Department of Chemistry, Georgetown University, 37th and O Streets NW, Washington, D.C. 20057, United States

S Supporting Information

ABSTRACT: New insights into the formation chemistry of chalcogenate-protected metal nanoparticles (NPs) synthesized via the well-known Brust–Schiffrin two-phase method are presented here. On the basis of Raman, NMR, and surface plasmon resonance characterizations, it is concluded that, before the formation of any metal–chalcogen bonds, metal nucleation centers/NPs are first formed inside the inverse micelles of the tetrabutylammonium bromide in the organic solvent, where the metal ions are reduced by NaBH₄. The ensuing formation of the metal–chalcogen bonds between the naked metal NPs inside the micelles and the organochalcogen ligands in the organic solvent is the mechanism by which the further growth of the metal core can be controlled. This proposed mechanism is further examined in the formation of Ag and Cu NPs.

Since the first synthesis of thiolate-protected Au NPs reported in 1994,¹ the Brust–Schiffrin (BS) two-phase synthetic method has become the most widely used synthesis of small Au NPs^{2–5} as well as Ag, Cu, and other metal NPs.^{6–11} Since it was shown by quantum calculations that other chalcogen–metal contacts might achieve better conductance than S,¹² Au NPs with Se or Te as anchoring element have also been prepared by the revised BS method.^{13–16} In order to obtain uniform metal NPs with size control, extensive efforts have been devoted to the stepwise investigation of the BS two-phase synthesis. Many groups^{17–20} tried to identify the precursors of metal ions prior to the addition of NaBH₄, but their exact form remains debatable. The widely accepted assumption has been that the addition of thiol reduces Au(III) to Au(I) and forms [Au(I)SR]_n-like polymers.^{4,5} Yet the most recent, thought-provoking results from Lennox and co-workers have shown otherwise.²⁰ On the basis of a quantitative solution ¹H NMR study of the metal salts, the phase-transfer agent tetrabutylammonium bromide (TOAB), and the thiol, they have demonstrated that the metal precursor before the addition of the reductant is TOA metal(I) halide complex [TOA]–[AuX₂], and not [M(I)SR]_n-like polymers. However, since the former does not involve a metal (M)–sulfur (S) bond, what happens and at what stage the Au–S bond is formed after the addition of NaBH₄ during the BS synthesis remain largely unresolved.

We report here detailed Raman, NMR, and surface plasmon resonance (SPR) spectroscopic studies of the reaction solutions after the sequential additions of thiol (or ligands in general) and NaBH₄ after the phase transfer and separation. Since our systematic Raman study showed no M–S bond formation in the

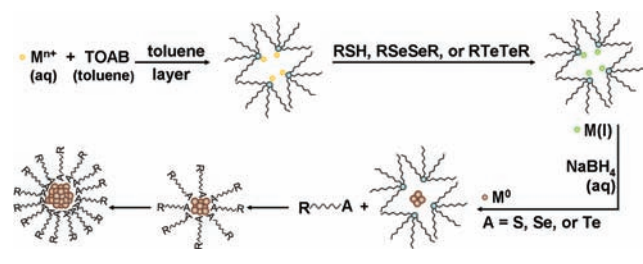
reaction solutions before the NaBH₄ addition, we confirmed that the [M(I)SR]_n-like polymers in which a M–S bond is expected are *not* the metal-ion precursors. While this observation renders strong support to Lennox's proposition,²⁰ it nonetheless raises an intriguing but also fundamentally important question as to when the M–S bond is formed, because this is the key step by which the metal NP growth and size are controlled. To answer this question, a reversed synthetic route in which reduction by NaBH₄ takes place before the addition of thiols (or other ligands) was devised and employed. This reversed (with respect to the original BS synthesis) procedure was inspired by the ¹H NMR observation of the possible existence of inversed micelles in the reaction solutions (*vide infra*). A time variable between the NP formation right after the reduction and the subsequent binding of the ligand was thus introduced and expected to help delineate the process. On the basis of careful analysis of the comparative spectroscopic results obtained in both the reversed and the BS syntheses of metal NPs, we propose a general metal NP formation mechanism for the latter, as outlined in Scheme 1. Its salient point is that the M–S bond is formed *after* the formation of the metal NPs in the inverse micelles. This general mechanism is shown to apply also to the formation of the Ag and Cu NPs. As we will show below, unraveling this mechanism makes it possible to use the stirring time prior to the addition of thiol to control the sizes of metal NPs. The reversed synthetic route also works with Se- and Te-containing ligands.

Whether or not the M–S bonds were formed in the reaction solution of a typical BS two-phase reaction before the addition of NaBH₄ was monitored by Raman spectroscopy. The typical procedure for mixing all precursors is as follows: a hydrogen tetrachloroaurate (HAuCl₄, 0.05 mmol) aqueous solution (0.35 mL) was mixed with a TOAB (0.15 mmol) toluene solution (5.0 mL) and stirred until the color of the aqueous phase disappeared. The bottom colorless layer was then discarded, and dodecanethiol (C₁₂SH, 0.10 mmol) was added to the separated wine-red toluene (or benzene) layer. After being stirred for 1 h, a clear, colorless solution was obtained, even in the cases of higher RSH/Au(III) ratios (such as RSH/Au = 3 or 5), which is different from Whetten's procedure in which no phase separation was done before the addition of thiols and NaBH₄.⁶ Before the Raman measurement, most solvent was removed by rotary evaporation under vacuum. The Raman spectrum of the fresh mixture, i.e., the concentrated organic solution of HAuCl₄, 3 equiv of TOAB, and 2 equiv of dodecanethiol, is compared with those of relevant reference materials in Figure 1. The absence of the peak at

Received: November 22, 2010

Published: January 26, 2011

Scheme 1. Mechanism for Chalcogenate-Protected Metal NP Synthesis by the Brust–Schiffrin Method



$\sim 327 \text{ cm}^{-1}$, which is a manifestation of the Au–S bond formation as demonstrated clearly in Figure 1c of the self-assembled dodecanethiol on the rough Au electrode and Figure 1d of the $[\text{Au(I)SR}]_n$ -like polymer obtained by following Lee's one-phase method,²¹ demonstrates convincingly that the addition of thiol to the separated Au(III) + TOAB solution did not form any Au–S bond. The disappearance of the S–H vibration at 2568 cm^{-1} and the new tiny peak at 525 cm^{-1} of $\text{C}_{12}\text{S–SC}_{12}$ (Figure 1e), together with the new peak at 2.57 ppm in the ^1H NMR spectrum (Figure S1a, see Supporting Information, SI), indicate that the reduction of Au(III) by RSH did occur as suggested in Whetten's early work.¹⁸ The peak at 209 cm^{-1} can be assigned to the Au– Br_2^- stretching vibration.²² Since no Au–S vibrational peak was observed (also see Figures S2 and S3 in the SI for the Ag and Cu systems, respectively), it confirms that the metal-ion precursor after the addition of thiol was not a $[\text{M(I)SR}]_n$ -like polymer, but a $[\text{TOA}][\text{M(I)X}_2]$ complex.²⁰

The ^1H NMR spectra of the TOAB + Au(III) solutions with different TOAB/Au(III) ratios were also recorded (Figure 2) to provide further structural information about the solutions. The large downfield shift of the H_2O peaks in spectra c–f as compared to the free H_2O peaks (spectra a and h) was indicative of the encapsulation of H_2O in the inverse micelle structures formed by TOAB. In addition, the peaks observed in the DLS spectra of the TOAB + Au(III) solutions before and after the addition of thiols (Figure S4, SI) are consistent with the existence of the inverse micelle structures, although these peaks were usually assigned to $[\text{M(I)SR}]_n$ -like polymers in the literature.¹⁹

Now the questions become at what stage in the BS synthesis are the Au–S bonds formed and how are they formed? Just as some previous literature showed,^{23,24} we have observed that the addition of NaBH_4 to the mixture of TOAB and HAuCl_4 without the presence of any ligand can also form metal NPs due to the presence of micelles,²⁵ despite a lack of long-term stability. Therefore, the observation of micelle-encapsulated water in the ^1H NMR spectra (Figure 2) in the separated organic phase led us to hypothesize that the following may happen stepwise in the BS two-phase synthesis after the addition of NaBH_4 . As shown above, the organic layer after the phase separation and the thiol addition contains the TOAB micelles of $[\text{TOA}][\text{M(I)X}_2]$ complex. The subsequent addition of NaBH_4 first reduces the metal ions that form the “naked”, micelle-encapsulated (but not TOAB directly capped) Au NPs. The ligands (the thiolate generated from the reduction of disulfide and the unreacted thiol) in the organic solvent then diffuse through the TOA shell and form the Au–S bonds at the water/organic solvent interface, by which the ligand-protected metal NPs are formed, as illustrated in Scheme 1.

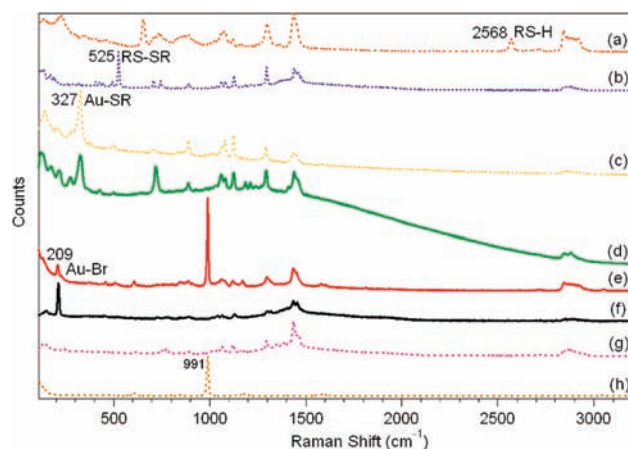


Figure 1. Raman spectra of (a) dodecanethiol, (b) didodecyl disulfide, (c) dodecanethiol self-assembled on rough Au electrode, (d) synthesized $[\text{AuSR}]_n$ -like polymer, (e) the concentrated C_6H_6 layer of HAuCl_4 and 3 equiv of TOAB after the addition of 2 equiv of dodecanethiol, (f) synthesized $[\text{TOA}][\text{AuBr}_2]$ complex, (g) TOAB, and (h) C_6H_6 .

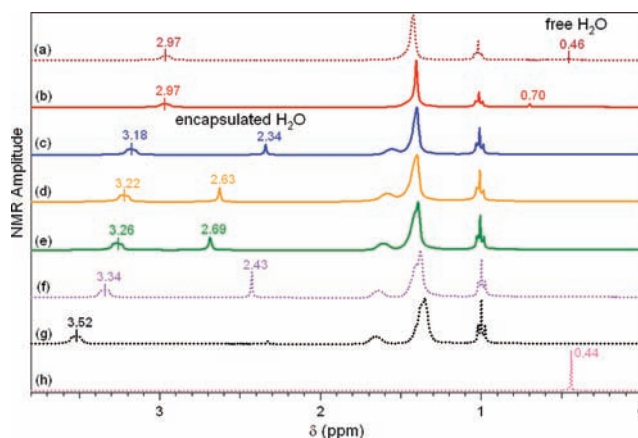


Figure 2. ^1H NMR spectra of (a) $[\text{TOA}][\text{AuBr}_4]$ complex (0.025 mmol) in C_6D_6 ; of the organic layer of TOAB (0.03 mmol) in C_6D_6 mixed with (b) HAuCl_4 (0.03 mmol) aqueous solution (0.21 mL), (c) HAuCl_4 (0.015 mmol) aqueous solution (0.105 mL of H_2O), (d) HAuCl_4 (0.01 mmol) aqueous solution (0.07 mL), and (e) HAuCl_4 (0.006 mmol) aqueous solution (0.042 mL); (f) of the organic layer of TOAB (0.03 mmol) in C_6D_6 mixed with 0.105 mL of H_2O ; (g) of TOAB (0.03 mmol) in C_6D_6 ; and (h) of the organic layer of C_6D_6 mixed with 0.105 mL of H_2O . (Note: 0.80 mL of C_6D_6 for each sample and 0.1421 M of the stock HAuCl_4 aqueous solution were used.)

To test the above hypothesis, we employed a reversed synthetic route for the metal NPs formation as follows. A HAuCl_4 (0.1 mmol) aqueous solution (0.7 mL) was first mixed with a TOAB (0.3 mmol) toluene solution (10 mL) and stirred until the aqueous phase became colorless. As shown in Figure 2, micelles were formed in this mixture. A fresh NaBH_4 aqueous solution (1 mL) was then poured into the mixture. After 10 s of stirring, as the color of the mixture changed from the initial wine-red to red-brown, which indicated the formation of the micelle-encapsulated Au NPs. A C_{12}SH (0.3 mmol) toluene solution (2 mL) was added quickly into the solution to form the final stable, ligand-protected ultrasmall Au NPs with good size distribution ($1.7 \pm 0.3 \text{ nm}$), as confirmed by the SPR spectrum and the TEM image (Figure 3a). Notice that if the BS

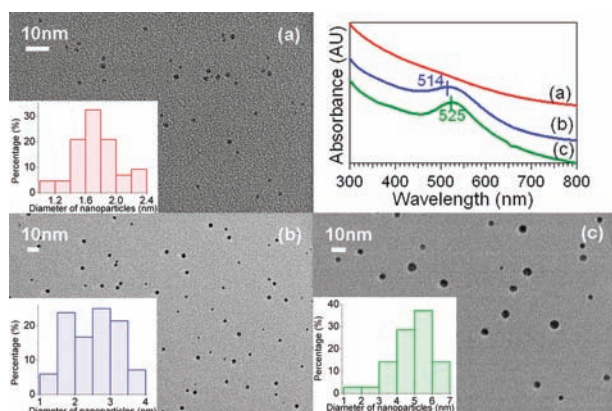


Figure 3. TEM images with size distribution and UV–visible spectra of the dodecanethiolate-protected Au nanoparticles obtained through our reversed synthetic route with stirring times of (a) 10 s, (b) 10 min, and (c) 24 h before the addition of thiols.

two-phase method was followed with exactly the same amount of materials, Au NPs of the same size were obtained (Figure S5, SI), strongly suggesting that they follow the same NP formation mechanism.

If the proposed mechanism is correct, then increasing the stirring time before the thiol addition while keeping other parameters constant is expected to increase the probability of collision between micelles,²⁵ in which the initially formed smaller Au NPs would grow larger. This was indeed observed when the stirring time was increased from 10 s to 10 min and 24 h: larger Au NPs (2.5 ± 0.7 and 4.8 ± 1.1 nm, respectively) were formed, as shown by the corresponding SPR spectra and TEM images (Figure 3b,c). The same procedure was also applied to forming the Ag and Cu NPs (Figure S6, SI). As observed for the Au NPs, the UV–vis spectra of Ag and Cu NPs also showed the same SPR peaks as those prepared via the typical BS two-phase synthesis (Figure S7, SI), suggesting strongly again the same NP formation mechanism in both synthetic routes. The NP size controlling effect of the thiol/Au ratio that has been widely used in the BS two-phase synthesis^{2,18} can also be achieved in the reversed route, as illustrated in Figures S8 and S9 (SI).

Additionally, it was observed that disulfide could also be used as ligand in both synthetic routes and produced Au NPs of similar size (Figure S10, SI), which was different from that obtained using thiol as ligands and with the same S/Au ratio. Consequently, the fact that thiol and disulfide coexist before the reduction with NaBH_4 in a typical BS two-phase synthesis²⁰ more likely one of the major reasons why the size distribution of the fresh NPs synthesized by the BS two-phase method is not narrow and postsynthetic treatment is needed.^{4,5} Moreover, since disulfide cannot reduce Au(III), these results showed that Au(I) is not a necessary precursor for forming Au NPs.

We next compared the Au NPs formation processes using dialkyl diselenide (RSeSeR) and dialkyl ditelluride (RTeTeR) as ligands in the BS two-phase and the reversed synthetic routes. The ^1H NMR spectra of the reaction solution after adding RSeSeR or RTeTeR were recorded (Figure S11, SI). The disappearance of the triplet peak at 2.75 (2.95) ppm due to the proton in $-\text{CH}_2-\text{Se}(\text{Te})-$ suggested strongly that the RSe–SeR (RTe–TeR) bond was broken via reacting with Au(III). Although the exact chemical state of the organo-chalcogen species after the bond breaking is currently under investigation, the similar proton NMR

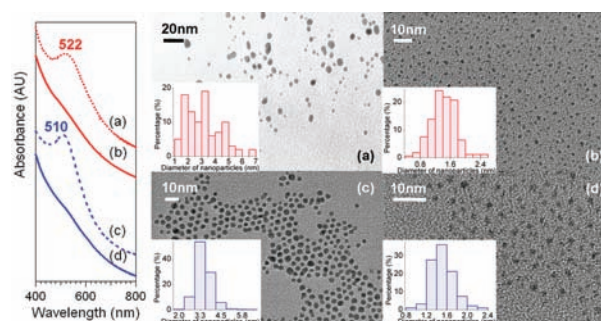


Figure 4. TEM images with size distributions and UV–vis spectra of Au nanoparticles protected with (a,b) Se-containing ligands and (c,d) Te-containing ligands by Brust–Schiffrin two-phase method (dot line) vs our reversed synthetic route (solid line). (Note: (c) after centrifugation.)

spectra (Figure S11c,e,g) of the respective reaction solutions after the addition of the ligands suggest that all of them had a similar precursor species of Au ions, i.e., $[\text{TOA}][\text{AuX}_2]$. It has also been observed that the BS two-phase method generally fails to produce <2 nm Au NPs with ditelluride, and the size distribution is usually poor for diselenide (Figure 4a,c, 3.4 ± 0.5 and 3.1 ± 1.2 nm, respectively). On the other hand, the reversed synthetic route shows a superior performance in these cases and can easily produce <2 nm Au NPs with good size distribution (Figure 4b,d 1.4 ± 0.3 and 1.5 ± 0.2 nm, respectively).

In summary, we have reported above several observations of general importance in understanding how metal NPs are formed in the popular BS two-phase synthesis. First, our Raman spectroscopic investigation (Figure 1) showed that, after thiol addition, no M–S bonds were formed. This was demonstrated by the control experiment of Raman measurement on the synthesized $[\text{M}(\text{I})\text{SR}]_n$ -like polymers. Notably, the Raman measurement showed that the $[\text{M}(\text{I})\text{SR}]_n$ -like polymers did involve the M–S bonds (Figure 1d). These observations provide independent spectroscopic confirmation of the recent work by Lennox and co-workers²⁰ in which they elegantly showed that the metal precursor before the NaBH_4 reduction in the BS two-phase method is not the generally believed $[\text{M}(\text{I})\text{SR}]_n$ -like polymer but the $[\text{TOA}][\text{MX}_2]$ complex. Second, on the basis of the observation of the micelle-encapsulated water that hosts the metal ion complex (Figures 2 and S4) and the success of the reversed synthetic route (Figures 3 and 4), we have proposed a general metal NPs formation mechanism applicable to the BS two-phase method as illustrated in Scheme 1. In other words, it is basically an inverse micelle-based synthetic procedure. Third, we have also shown that the reversed synthetic route generally offers better control in forming different metal (Au, Ag, and Cu) NPs with different organo-chalcogen ligands as the stabilizers. A similar process was reported previously, but digestive ripening was necessary to obtain the homogeneous larger (~ 5 nm) Au NPs.²⁶ The emergence of these new mechanistic insights will help synthesize organo-chalcogen-stabilized metal NPs with better control.

■ ASSOCIATED CONTENT

S Supporting Information. Experimental and synthetic details, DLS spectra, Raman spectra, UV–vis spectra, ^1H NMR spectra, and TEM images. This material is available free of charge via the Internet at <http://pubs.acs.org>.

AUTHOR INFORMATION

Corresponding Author

yyt@georgetown.edu

ACKNOWLEDGMENT

This work is supported by grants from the National Science Foundation (CHE 0456848 and CHE 0702859). G.Y. was a summer exchange undergraduate student from Fudan University, Shanghai, China. The authors thank Ms. Monica Pate and Mr. Yangwei Liu for assisting with some syntheses reported, Ms. Maki Nishida and Prof. Ed Van Keuren from the Department of Physics at Georgetown University for assisting with the DLS measurements, and UMD NISP Lab for use of its TEM facility.

REFERENCES

- (1) Brust, M.; Walker, M.; Bethell, D.; Schiffrin, D. J.; Whyman, R. *J. Chem. Soc., Chem. Commun.* **1994**, 801–802.
- (2) Templeton, A. C.; Wuelfing, W. P.; Murray, R. W. *Acc. Chem. Res.* **2000**, *33*, 27–36.
- (3) Murray, R. W. *Chem. Rev.* **2008**, *108*, 2688–2720.
- (4) Funston, A. M.; Mulvaney, P.; Murray, R. W. *Langmuir* **2009**, *25*, 13840–13851.
- (5) Jin, R. *Nanoscale* **2010**, *2*, 343–362.
- (6) Murthy, S.; Bigioni, T. P.; Wang, Z. L.; Khoury, J. T.; Whetten, R. L. *Mater. Lett.* **1997**, *30*, 321–325.
- (7) Kang, S. Y.; Kim, K. *Langmuir* **1998**, *14*, 226–230.
- (8) Garitaonandia, J. S.; Insausti, M.; Goikolea, E.; Suzuki, M.; Cashion, J. D.; Kawamura, N.; Ohsawa, H.; Gil de Muro, I.; Suzuki, K.; Plazaola, F.; Rojo, T. *Nano Lett.* **2008**, *8*, 661–667.
- (9) Dadgostar, N.; Ferdous, S.; Henneke, D. *Mater. Lett.* **2010**, *64*, 45–48.
- (10) Gopidas, K. R.; Whitesell, J. K.; Fox, M. A. *Nano Lett.* **2003**, *3*, 1757–1760.
- (11) Zelakiewicz, B. S.; Lica, G. C.; Deacon, M. L.; Tong, Y. Y. *J. Am. Chem. Soc.* **2004**, *126*, 10053–10058.
- (12) Di Ventura, M.; Lang, N. D. *Phys. Rev. B* **2001**, *65*, 045402.
- (13) Brust, M.; Stuhr-Hansen, N.; Norgaard, K.; Christensen, J. B.; Nielsen, L. K.; Bjornholm, T. *Nano Lett.* **2001**, *1*, 189–191.
- (14) Yee, C. K.; Ulman, A.; Ruiz, J. D.; Parikh, A.; White, H.; Rafailovich, M. *Langmuir* **2003**, *19*, 9450–9458.
- (15) Zelakiewicz, B. S.; Yonezawa, T.; Tong, Y. Y. *J. Am. Chem. Soc.* **2004**, *126*, 8112–8113.
- (16) Li, Y.; Silvertown, L. C.; Haasch, R.; Tong, Y. Y. *Langmuir* **2008**, *24*, 7048–7053.
- (17) Alvarez, M. M.; Khoury, J. T.; Schaaff, T. G.; Shafigullin, M.; Vezmar, I.; Whetten, R. L. *Chem. Phys. Lett.* **1997**, *266*, 91–98.
- (18) Schaaff, T. G.; Shafigullin, M. N.; Khoury, J. T.; Vezmar, I.; Whetten, R. L.; Cullen, W. G.; First, P. N.; Gutierrez-Wing, C.; Ascencio, J.; Jose-Yacamán, M. J. *J. Phys. Chem. B* **1997**, *101*, 7885–7891.
- (19) Zhu, M.; Lanni, E.; Garg, N.; Bier, M. E.; Jin, R. *J. Am. Chem. Soc.* **2008**, *130*, 1138–1139.
- (20) Goulet, P. J. G.; Lennox, R. B. *J. Am. Chem. Soc.* **2010**, *132*, 9582–9584.
- (21) Kim, J.-U.; Cha, S.-H.; Shin, K.; Jho, J. Y.; Lee, J.-C. *J. Am. Chem. Soc.* **2005**, *127*, 9962–9963.
- (22) Braunstein, P.; Clark, R. J. H. *J. Chem. Soc., Dalton Trans.* **1973**, 1845–1848.
- (23) Fink, J.; Kiely, C. J.; Bethell, D.; Schiffrin, D. J. *Chem. Mater.* **1998**, *10*, 922–926.
- (24) Thomas, K. G.; Zajicek, J.; Kamat, P. V. *Langmuir* **2002**, *18*, 3722–3727.
- (25) Pileni, M. P. *J. Phys. Chem.* **1993**, *97*, 6961–6973.
- (26) Lin, X. M.; Sorensen, C. M.; Klabunde, K. J. *J. Nanopart. Res.* **2000**, *2*, 157–164.